

QSAR analysis of antimicrobial and haemolytic effects of cyclic cationic antimicrobial peptides derived from protegrin-1

Vladimir Frečer*

*Cancer Research Institute, Slovak Academy of Sciences, Bratislava SK-83391, Slovakia
International Centre for Science and High Technology, UNIDO, AREA Science Park, Trieste I-34012, Italy*

Received 2 March 2006; revised 12 April 2006; accepted 3 May 2006

Available online 22 May 2006

Abstract—In this paper we quantitatively analyse antimicrobial and haemolytic activities of porcine protegrin-1 (PG-1) mimetics—cyclic cationic peptides with β -hairpin fold synthesised by Robinson et al. [*Bioorg. Med. Chem.* **2005**, *13*, 2055]. The presented QSAR models, which use molecular properties related to possible mechanisms of cell membrane disruption that can be easily calculated from available data on amino acids, rationalize the relationships between sequences and antimicrobial and haemolytic potencies of the cyclic peptides. The best models obtained by application of genetic function approximation algorithm correlate antimicrobial potencies to the peptide's charge and amphipathicity index, while the haemolytic effect correlates well with the lipophilicity of residues forming the nonpolar face of the β -hairpin. The models permit selection of site-directed residue substitutions leading to simultaneous optimization of antimicrobial and haemolytic potencies. Examples of such residue substitutions in the nonpolar face of a symmetric cyclic β -hairpin PG-1 analogue with an ideal amphipathic structure are given.

© 2006 Elsevier Ltd. All rights reserved.

1. Introduction

Antibiotic-resistant bacterial strains represent a global health problem, thus an urgent need exists to develop new antibiotics with novel mechanism of action.¹ Cationic antimicrobial peptides form a vital component of the innate immunity against microbial infections.² They are being considered as potential drugs for treatment of infections because they are extremely fast acting^{3,4} and their mechanism of action, which generally involves disruption of microbial membranes, is thus less likely to induce drug resistance.^{5–7} Widely distributed in plants and animals, antimicrobial peptides vary in amino acid composition, structure and size. However, despite their diversity, most antimicrobial peptides share some common features that include net positive charge and amphipathic character, which segregates hydrophilic and hydrophobic residues to opposite faces of the molecule.^{3,6} Although the precise mode of their action is not fully understood, it was proposed that the cationic peptides initially bind to negatively charged lipopolysac-

charides and phospholipids of the outer leaflet of bacterial membrane, accumulate and aggregate on the membrane surface and finally permeabilize/disintegrate the bacterial membrane through various possible mechanisms including pore formation.^{8–10} Nuclear magnetic resonance studies revealed that a minimum peptide to membrane lipid ratio must be achieved before a cationic peptide can lyse a cell.¹¹ It has been recently pointed out that membrane disruption may not be the ultimate mechanism of rapid microbial killing by antimicrobial peptides. Several observations suggest that translocated peptides can block cell-wall, nucleic acid and protein synthesis as well as inhibit enzymatic activity of bacteria.^{2,12} Nevertheless, permeation/disintegration of the bacterial membrane remains to be an important element of the antimicrobial effect of cationic peptides.

As a harmful side effect many antimicrobial peptides lyse the membranes of mammalian cells causing thus haemolytic and/or cytotoxic effects in humans,^{8,13} which hinder their wider utilization. Therefore, additional research efforts are needed to understand how to discriminate the antimicrobial and haemolytic effects of cationic peptides.

Numerous laboratories have been involved in the development of antimicrobial peptides with various secondary structures using mainly random or combinatorial

Keywords: Cationic antimicrobial peptides; QSAR analysis; Genetic function approximation algorithm; Molecular properties; Optimisation of antimicrobial and haemolytic effects.

* Tel.: +421 2 5932 7113; fax: +421 2 5932 7250; e-mail: exonfrec@savba.sk

design approaches.^{7,14–20} For rational design of potent and selective antimicrobial peptide sequences it is useful to establish quantitative structure–activity relationships (QSAR) based on descriptors that are related to the mechanism of their action. The mechanism of bacterial membrane disruption may proceed through several consecutive steps, which may involve the following molecular properties: (i) positive charge—attachment to anionic outer layer of bacterial membrane, (ii) amphipathicity—aggregation on the membrane surface and (iii) lipophilicity—permeation into lipophilic membrane interior.^{3,8–10} These properties have been previously used to successfully explain antimicrobial potency of some cationic peptides.^{14,21–24}

Protegrins are short natural cationic peptides isolated from porcine leukocytes, which display a broad spectrum of antimicrobial effects against Gram-negative, Gram-positive bacteria, yeasts and fungi.^{14,25–27} They are similar to other defensins. Protegrin-1 (PG-1) with 18 amino acid residues forms a rigid antiparallel two-stranded β -sheet linked by a short two-residue loop segment and stabilised by two disulfide bridges (Fig. 1). PG-1 binds lipopolysaccharides and lipid A,²⁸ inserts into anionic phospholipid membranes and forms oligomeric aggregates.^{29,30} Previous studies on PG-1 mimetics indicated that linear analogues exhibit reduced antimicrobial activity, while analogues retaining the cross-linked β -hairpin secondary structure conserve their potency in spite of various substitutions.^{27,31} Large number of amino acid substitutions are tolerated by the PG-1 structure, implying that overall structural features such as amphipathicity, charge and shape are more important to activity than the presence of specific amino acids. The total number of cationic residues and the amphipathicity of the β -hairpin determine the activity; however, the analogues displayed relatively high toxicity to mammalian cells.^{14,27} Langham et al.³² studied interactions of PG-1 with sodium dodecylsulfate and dodecylphosphocholine micelles as models of bacterial and mammalian membranes by molecular dynamics simulations at the atomic scale of resolution. In both micelle types the arginines of PG-1 strongly interacted with

the lipid headgroups, but acquired different positions and orientations with respect to the membrane interior, which can be related to different effects of PG-1 on bacterial and mammalian cells.

Robinson et al.³³ have synthesised and tested a series of PG-1 mimetic cyclic peptides (Fig. 1), which displayed good antimicrobial activities and reduced haemolytic effects. Structure–activity study of the series containing 97 analogues of the lead peptide R1: *cyclo*-(Leu-Arg-Lys-Lys-Arg-Arg-Trp-Lys-Tyr-Arg-Val-D-Pro-Pro-) by performing single site residue substitutions showed that the antimicrobial activity was tolerant to a large number of substitutions. Some analogues showed slightly improved antimicrobial activities, whereas other substitutions caused large increases in the haemolytic activity.³³ Both enantiomeric forms of R1 showed similar antimicrobial potencies, which is a typical feature of cationic peptides targeting the cell membrane.³⁴ Unfortunately, the study did not offer deeper insight into the structure–activity relationships between the peptide sequences or molecular properties and the observed biological effects. It has neither managed to develop analogues that would be significantly more potent and at the same time less haemolytic than the starting lead peptide R1.

Ostberg and Kaznessis²⁴ carried out an extensive QSAR study of antimicrobial, haemolytic and cytotoxic effects of protegrin analogues using descriptors computed from three-dimensional (3D) homology models of PG-1. They established a separate QSAR model for each activity and each strain tested with regression equations containing up to five relatively complex molecular descriptors. Unfortunately, their models neither allow easy interpretation nor offer clear guidelines for peptide optimisation or design.

In this paper, we have quantitatively analysed the antimicrobial and haemolytic activities of the cationic peptide sequences of Robinson et al.³³ in terms of simple additive molecular properties related to the general mechanism of cell membrane disruption. The presented

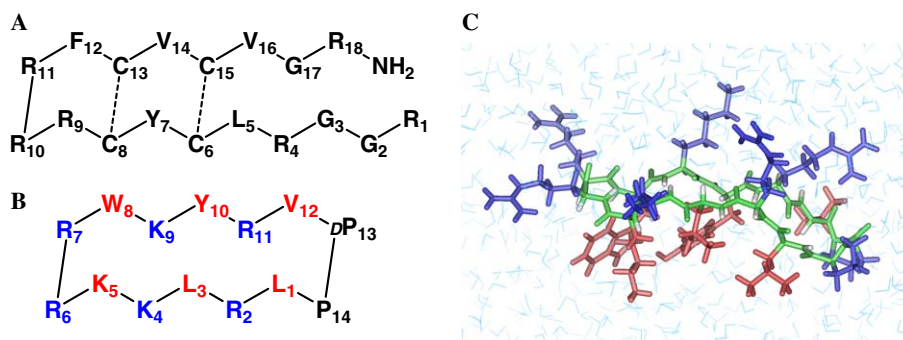


Figure 1. Cyclic β -hairpin peptides—analogs of protegrin 1. (A) Protegrin-1. (B) The polar face of the cyclic β -hairpin lead peptide R1 of Robinson et al.³³ is formed by the side chains of cationic residues 2, 4, 6, 7, 9, 11 and the prolines 13 and 14 (blue colour), while the nonpolar face is made of residues 1, 3, 5, 8, 10 and 12 (red colour) with predominant lipophilic/aromatic character. (C) 3D model of solvated peptide R1 in stick representation (colouring scheme: peptide backbone—green, nonpolar face side chains—red, polar face side chains—dark blue and water molecules—light blue). Due to the anti-parallel β -sheet and structure of the backbone the cyclic peptide forms two distinct faces with side chains of residues occupying the space mainly on the opposite sides of the backbone scaffold.

QSAR models obtained by the application of genetic function approximation algorithm³⁵ rationalize the relationship between peptide sequences and antimicrobial and haemolytic effects of the PG-1 mimetics. The QSAR models permit selection of site-directed residue substitutions leading to simultaneous optimisation of the antimicrobial and haemolytic potencies. Examples of such residue substitutions in the polar and nonpolar faces of altered symmetric cyclic β -hairpin PG-1 analogues with ideal amphipathic structure are given.

2. Results and discussion

2.1. QSAR analysis

In the β -hairpin-like secondary structure of the lead peptide R1 of Robinson et al.³³ it is possible to formally distinguish between cationic residues and prolines forming the polar face (residues 2, 4, 6, 7, 9, 11, 13 and 14) and residues with a lipophilic/aromatic character (residues 1, 3, 5, 8, 10 and 12) forming the nonpolar face of the cyclic peptide (Fig. 1). Lysine 5 and prolines 13 and 14 form an exception from this classification and represent a deviation of R1 from an ideal cyclic amphipathic motif. Nevertheless, due to the anti-parallel β -sheet structure of the backbone the side chains of the residues occupy the space roughly on opposite sides (faces) of the backbone scaffold (Fig. 1C). This is valid also for the analogues obtained by systematic single residue substitutions in the sequence of R1.

The R1 lead displayed minimal inhibitory concentrations (MICs) against three bacterial strains tested (*Escherichia coli*, *Pseudomonas aeruginosa* and *Staphylococcus aureus*) of 12.5, 6.5 and of 12.5 $\mu\text{g/mL}$ and percentage of haemolysis (%Hem) of human red blood cells of 1.4% at a concentration of 100 $\mu\text{g/mL}$. Correlations between MICs of the R1 analogues in the individual species tested are shown in Table 1. Low off diagonal R^2 values characterize poor correlation of the MICs between individual species and render the analysis of the antimicrobial effect complicated. Therefore, we have averaged the values of MIC over the panel of bacterial strains tested to facilitate the assessment of the overall antimicrobial effect of the peptides. QSAR analysis that involves the averaged MIC_a reflects better the antibacterial potency of a class of peptides than analyses based on MICs against the individual strains, where the actual effect is strongly dependent on the bacterial membrane

composition, cell growth rate and life cycle of the particular strain. The MIC_a averages these factors and underlines the role of the peptide sequence and structure in the achieved antimicrobial effect.²³ Moreover, development of QSAR models for PG-1 analogues that are active against wide spectrum of Gram-negative and Gram-positive bacteria^{14,25–27} is preferable to structure–activity models applicable only to a single individual strain.

Within the homogeneous series of 97 R1 analogues of the same length and structure the MIC_a ranged between 5.2 and 83.3 $\mu\text{g/mL}$, while the range of %Hem stretched between 0.1 and 57.6% (Table 2).³³ Simultaneous substitutions of two or more residues would most probably expand the ranges of the observed potencies even further.

To rationalize why a conservative single or double mutation can sometimes significantly and sometimes selectively alter the antimicrobial and haemolytic potencies within this homogeneous series, we have analysed the relationships between sequences and observed bioactivities in terms of physico-chemical molecular properties of the peptides. The selected properties, which characterize peptide's charge, lipophilicity, amphipathicity, size, shape and flexibility included the following descriptors: charge (Q), overall lipophilicity (L), lipophilicity of polar and nonpolar faces (P and N), surface areas of polar and nonpolar faces (S_P and S_N), molecular mass of the polar and nonpolar faces (M_{WP} and M_{WN}), count of small lipophilic, highly lipophilic and aromatic residues forming the nonpolar face (C_{SL} , C_{HL} and C_{AR}), total number of hydrogen bond donor and acceptor centres (HB_{don} and HB_{acc}), total number of rotatable bonds (RotBon) and various amphipathicity descriptors (P/L , P/N , L/N , Q/L , Q/N , S_P/S_N , M_{WP}/M_{WN} , Q/C_{SL} , Q/C_{HL} and Q/C_{AR}). For definition of the descriptors, see Section 4. These simple additive molecular descriptors can be easily derived from peptide sequences and tabulated amino acid properties (Table 3).^{39,40} The descriptors do not fully describe 3D structure of the analogues, they mainly reflect the peptide sequence and location of a residue within the polar or nonpolar face. Although conformational flexibility of the R1 analogues in solution may be high, we may assume that the conformation-stabilizing features (Pro₁₃ and Pro₁₄)³³ as well as a structure-inducing effects in the proximity to the anionic bacterial membrane surface of bacteria will favour the amphipathic β -hairpin secondary structure of the

Table 1. Correlation of antimicrobial and haemolytic activities between species

	R^{2a}			
	MIC <i>E. coli</i>	MIC <i>P. aeruginosa</i>	MIC <i>S. aureus</i>	%Hem <i>Haemocytes</i>
MIC <i>E. coli</i>	1	0.31	0.23	0.01
MIC <i>P. aeruginosa</i>		1	0.49	0.01
MIC <i>S. aureus</i>			1	0.11
%Hem <i>Haemocytes</i>				1

^a Squared correlation coefficient obtained by linear regression of the MIC (minimum inhibitory concentration in micrograms per milliliter) and %Hem (haemolytic activity in [%]) for 97 analogues of R1 antimicrobial peptide of Robinson et al.³³ The off diagonal R^2 values characterize correlation of MIC between the species and with the haemolytic effect.

Table 2. Range of antimicrobial and haemolytic potencies of R1 analogues^a

Pep.	Type	P.1	P.2	P.3	P.4	P.5	P.6	P.7	P.8	P.9	P.10	P.11	P.12	P.13	P.14	MIC _a ^b (μg/mL)	%Hem ^c (%)
R1	Original lead	Leu	Arg	Leu	Lys	Lys	Arg	Arg	Trp	Lys	Tyr	Arg	Val	Pro	Pro	10.4	1.4
R9	Most active	Cif ^d	Arg	Leu	Lys	Lys	Arg	Arg	Trp	Lys	Tyr	Arg	Val	Pro	Pro	5.2	11.5
R12	Least active	Orn ^d	Arg	Leu	Lys	Lys	Arg	Arg	Trp	Lys	Tyr	Arg	Val	Pro	Pro	83.3	0.7
R23	Least active	Leu	Arg	Orn	Lys	Lys	Arg	Arg	Trp	Lys	Tyr	Arg	Val	Pro	Pro	83.3	1.5
R64	Least active	Leu	Arg	Leu	Trp	Lys	Arg	Arg	Trp	Lys	Tyr	Arg	Val	Pro	Pro	83.3	4.0
R45	Least haemolytic	Leu	Arg	Leu	Lys	Lys	Arg	Arg	Trp	Lys	Orn	Arg	Val	Pro	Pro	50.0	0.1
R44	Most haemolytic	Leu	Arg	Leu	Lys	Lys	Arg	Arg	Trp	Lys	Cha ^d	Arg	Val	Pro	Pro	29.2	57.6

^a Sequences of cyclic antimicrobial peptides were taken from Robinson et al.,³³ for numbering of residues P.1–P.14, see Figure 1.^b Averaged minimal inhibitory concentration in units of micrograms per milliliter. MICs against *E. coli*, *P. aeruginosa* and *S. aureus* were taken from Robinson et al.³³^c Percentages of haemolysis of human red blood cells at peptide concentration of 100 μg/mL were taken from Robinson et al.³³^d Cha, L-cyclohexylalanine; Cif, L-4-chlorophenylalanine, and Orn, L-ornithine.**Table 3.** Side-chain descriptors of natural and unusual amino acids

No.	Amino acid ^a	Q ^b (e)	π _{FP} ^c	Hydro ^d	S ^e (Å ²)	M _w ^f (g/mol)	C _{SL} ^g	C _{HL}	C _{AR}	HB _{acc} ^h	HB _{don}	R.B. ⁱ
1	Abu	0	0.64 ^f	—	34.9	28.1	1	0	0	0	0	1
2	Ala	0	0.31	1.8	19.6	14.0	1	0	0	0	0	0
3	Arg+	+1	−1.01	−4.5	39.7	99.1	0	0	0	1	4	4
4	Asn	0	−0.60	−3.5	114.5	57.1	0	0	0	1	2	2
5	Asp−	−1	−2.57	−3.5	53.0	57.0	0	0	0	2	0	2
6	Bip	0	3.76	—	169.4	166.2	0	1	1	0	0	3
7	Cha	0	2.91	—	107.6	96.2	0	1	0	0	0	2
8	Chah	0	3.47	—	125.2	110.2	0	1	0	0	0	3
9	Cif	0	2.51	—	114.4	124.6	0	1	1	1	0	2
10	Cit	0	−0.19	—	103.0	100.1	0	0	0	1	3	5
11	Cys	0	1.54	2.5	37.6	46.1	1	0	0	1	1	2
12	Gln	0	−0.22	−3.5	71.7	71.1	0	0	0	1	2	3
13	Glu−	−1	−2.29	−3.5	61.6	71.1	0	0	0	2	0	3
14	Gly	0	0.00	−0.4	0.0	0.0	0	0	0	0	0	0
15	Hfe	0	2.31	—	111.5	104.2	0	1	1	0	0	3
16	His	0	0.13	−3.2	75.7	80.1	0	0	0	1	1	2
17	Ile	0	1.80	4.5	68.4	56.1	1	0	0	0	0	2
18	Leu	0	1.70	3.8	69.9	56.1	1	0	0	0	0	2
19	Lys+	+1	−0.99	−3.9	90.7	71.1	0	0	0	1	2	5
20	Met	0	1.23	1.9	78.2	74.1	1	0	0	1	0	3
21	Nal1	0	3.00	—	133.2	140.2	0	1	1	0	0	2
22	Nal2	0	3.00	—	141.8	140.2	0	1	1	0	0	2
23	Nle	0	1.76	—	76.4	56.1	1	0	0	0	0	3
24	Nva	0	1.19	—	54.0	42.1	1	0	0	0	0	2
25	Orn+	+1	0.40	—	71.2	57.1	0	0	0	1	2	4
26	Phe	0	1.79	2.8	92.2	90.1	0	0	1	0	0	2
27	Pro	0	0.72	−1.6	39.7	40.1	1	0	0	0	−1	0
28	Seb	0	2.53	—	128.7	120.2	0	1	1	1	0	4
29	Ser	0	−0.04	−0.8	26.7	30.0	0	0	0	1	1	2
30	Thr	0	0.26	−0.7	44.8	44.1	0	0	0	1	1	2
31	Tle	0	1.39	—	62.0	56.1	1	0	0	0	0	1
32	Trb	0	3.55	—	204.5	196.2	0	1	1	1	0	5
33	Trp	0	2.25	−0.9	121.1	129.2	0	1	1	0	1	2
34	Tyr	0	0.96	−1.3	102.0	106.1	0	0	1	1	1	3
35	Val	0	1.22	4.2	51.1	42.1	1	0	0	0	0	1

^a Abu, L-2-aminobutyric acid; Bip, L-4-biphenylalanine; Cha, L-cyclohexylalanine; Chah, L-homocyclohexylalanine; Cif, L-4-chlorophenylalanine; Cit, L-citrulline; Hfe, L-homophenylalanine; Nal1, L-1-naphthylalanine; Nal2, L-2-naphthylalanine; Nle, L-norleucine; Nva, L-norvaline; Orn, L-ornithine; Trb, L-(*O*-benzyl)tyrosine; Seb, L-(*O*-benzyl)serine; Tle, L-*tert*-leucine.^b Residue net charge based on pK_a constant of the side chain,³⁹ in units of electron charge [e].^c Experimental side chain lipophilicity parameter of natural amino acids: π_{FP} = log P_{o/w}(a.a.) − log P_{o/w}(Gly) taken from Fauchere and Pliska⁴⁰ where the log P_{o/w} is the interphase partitioning coefficient in *n*-octanol/water system. For unusual amino acids the value of π_{FP} was predicted from a regression fit to π_{CLOGP} parameter (for details, see Section 4).^d Hydrophathy of amino acids according to Kyte and Doolittle.⁴⁵^e Side-chain surface area was computed as a difference in the Connolly surfaces⁴² of amino acid and glycine: S = S_{Con}(a.a.) − S_{Con}(Gly) (for details, see Section 4).^f Molecular weight of residue side chain was computed as a difference between M_ws of amino acid and glycine: M_w = M_w(a.a.) − M_w(Gly).^g Count of small lipophilic residues (C_{SL}), highly lipophilic residues (π_{FP} > 2.0) (C_{HL}) and aromatic residues (C_{AR}).^h Number of proton donor (HB_{don}) and proton acceptor (HB_{acc}) atoms in the peptide capable of forming hydrogen bonds.ⁱ Number of rotatable (single nonaromatic) bonds in the peptide side chains.

analogues. This assumption is consistent with the finding that protegrins and their synthetic analogues, which contain 1 or 2 disulfide bridges constraining their backbone into the β -hairpin conformation, display in general higher antimicrobial potencies than their linear or nonconstrained counterparts.⁷

No single molecular property descriptor provided individually a satisfactory pairwise correlation with the averaged antimicrobial ($\log \text{MIC}_a$) or haemolytic ($\log \% \text{Hem}$) potencies (Table 4). Nevertheless, lipophil-

Table 4. Correlation of single descriptors with antimicrobial and haemolytic activities

Descriptor ^a	$\log \text{MIC}_a^b$		$\log \% \text{Hem}^b$	
	LOF ^c	R^{2d}	LOF ^c	R^{2d}
Q (è)	0.070	0.001	0.319	0.021
L	0.066	0.069	0.287	0.120
P	0.070	0.007	0.307	0.060
N	0.058	0.175	0.169	0.481
S (Å)	0.063	0.106	0.259	0.205
S_P (Å)	0.070	0.012	0.309	0.053
S_N (Å)	0.062	0.113	0.267	0.182
M_w (g/mol)	0.064	0.090	0.281	0.137
M_{wP} (g/mol)	0.070	0.006	0.324	0.008
M_{wN} (g/mol)	0.064	0.090	0.281	0.140
C_{SL}	0.070	0.001	0.323	0.009
C_{HL}	0.065	0.083	0.229	0.298
C_{AR}	0.066	0.068	0.309	0.053
HB_{don}	0.070	0.001	0.326	0.001
HB_{acc}	0.069	0.020	0.300	0.081
P/L	0.061	0.141	0.307	0.058
P/N	0.068	0.033	0.321	0.016
L/N	0.068	0.033	0.321	0.016
Q/L	0.059	0.161	0.303	0.073
Q/N	0.058	0.181	0.255	0.217
S_P/S_N	0.065	0.076	0.295	0.095
M_{wP}/M_{wN}	0.066	0.061	0.297	0.089
Q/C_{SL}	0.070	0.001	0.320	0.020
Q/C_{HL}	0.065	0.076	0.271	0.169
Q/C_{AR}	0.066	0.057	0.323	0.009
RotBon	0.070	0.001	0.319	0.021

^a Descriptors: Q , molecular charge; L , molecular lipophilicity; P , lipophilicity of the polar face residues; N , lipophilicity of the nonpolar face residues; S , solvent accessible surface area of the analogue; S_P , solvent accessible surface area of the polar face residues; S_N , solvent accessible surface area of the nonpolar face residues; M_w , molecular weight of the analogue; M_{wP} , molecular weight of residues forming the polar face; M_{wN} , molecular weight of residues forming the nonpolar face; C_{SL} , count of small lipophilic residues forming the nonpolar face; C_{HL} , count of highly lipophilic residues forming the nonpolar face; C_{AR} , count of aromatic residues forming the nonpolar face; HB_{don} , overall number of proton donors in the analogue; HB_{acc} , overall number of proton acceptors in the analogue; P/L , P/N , L/N , Q/L , Q/N , S_P/S_N , M_{wP}/M_{wN} , Q/C_{SL} and Q/C_{AR} are various amphipathicity descriptors expressed as a ratio of the above-defined properties of the polar face to the nonpolar face.

^b Logarithm of averaged minimal inhibitory concentration and of the percentages of haemolysis of human red blood cells at peptide concentration of 100 $\mu\text{g/mL}$.

^c Friedman's lack-of-fit (LOF) score³⁷ of single descriptors was obtained by linear regression to the $\log \text{MIC}_a$ and $\log \% \text{Hem}$ of 97 antimicrobial peptides tested by Robinson et al.³³

^d Squared correlation coefficients of single descriptors were obtained by linear regression to the $\log \text{MIC}_a$ and $\log \% \text{Hem}$ of 97 antimicrobial peptides tested by Robinson et al.³³

icity of the nonpolar face N and the amphipathicity parameter Q/N exhibited some relation to the antimicrobial activity, while N and the intercorrelated count of highly lipophilic residues in the nonpolar face (C_{HL}) appeared to be related to the haemolytic activity. This finding is consistent with previous QSAR studies which suggested that charge and amphipathicity correlate with MIC of cyclic cationic peptides and overall lipophilicity is crucial for the haemolytic activity.²³

A large set of QSAR models combining up to five descriptors in each correlation equation was prepared by genetic function approximation (GFA) algorithm³⁵ of the Cerius² package.³⁶ The fitness of each generated model was evaluated by using the lack-of-fit score.³⁷ The best performing QSAR model of the antimicrobial effect of R1 analogues comprises two descriptors, namely molecular charge Q and amphipathicity parameter Q/N , that is, the ratio of charge, which is determined by the cationic residues forming mainly the polar face and the lipophilicity of the nonpolar face, N (Fig. 2):

$$\log \text{MIC}_a = 1.291 - 0.180 \cdot Q + 1.438 \cdot Q/N \quad (1)$$

(number of observables $n = 97$, lack-of-fit score $\text{LOF} = 0.025$, squared correlation coefficient $R^2 = 0.623$, leave-one-out cross-validated squared correlation coefficient $R_{\text{cv}}^2 = 0.604$, Fischer test $F\text{-test} = 52.74$, standard error $\sigma = 0.164$, level of statistical significance $\alpha > 95\%$, number of removed outliers $n_o = 15$). Similar observation, which relates the antimicrobial effect of cationic peptides to the molecular charge and amphipathicity has been previously published by several laboratories.^{14,21–24} It is namely likely that peptides,

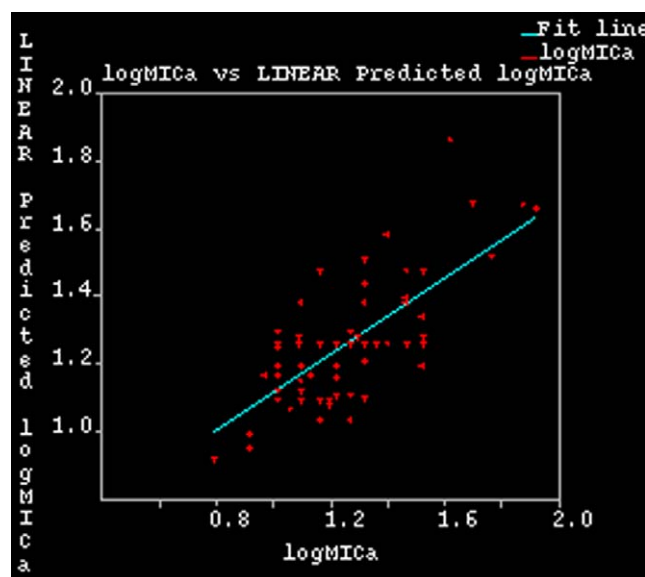


Figure 2. QSAR model of antimicrobial effect of cationic peptides—R1 analogues. The resulting regression equation: $\log \text{MIC}_a = 1.291 - 0.180 \cdot Q + 1.438 \cdot Q/N$ ($n = 97$, $R^2 = 0.62$, $R_{\text{cv}}^2 = 0.60$, $F\text{-test} = 52.74$, $\sigma = 0.164$, $\alpha > 95\%$, $n_o = 15$) relates averaged MIC_a (in $\mu\text{g/mL}$) against three bacterial strains (*Escherichia coli*, *Pseudomonas aeruginosa* and *Staphylococcus aureus*) to molecular charge (Q) and amphipathicity index (Q/N). The MICs were taken from Robinson et al.³³ Figure was obtained by QSAR module of Cerius².³⁶

which possess a balanced combination of positive charge and lipophilicity of a surface domain (nonpolar face) can be attracted to the bacterial membrane in a sufficient amount to aggregate and permeate/disintegrate the membrane triggering thus the antimicrobial effect.

The dependence of MIC_a on Q and N is depicted on Figure 3. The plot reveals that for the highly charged cationic R1 analogues the antimicrobial potency is less sensitive to the molecular charge (within interval $6e \leq Q \leq 8e$). It is, however, strongly dependent on the lipophilicity of the nonpolar face. The MIC_a can reach low concentrations for high values of N ($N \geq 10$), however, MIC_a grows quickly with the decreasing magnitudes of N ($N \leq 7.5$). Based on this QSAR model, the best variants of R1 lead should have their polar faces formed only by charged residues and the nonpolar faces only by highly lipophilic residues to display strong antimicrobial effect. Thus, any analogue with the same charge as the lead peptide R1 ($Q = 7e$) should show more potent antimicrobial activity than R1 if the lipophilicity of its nonpolar face $N \geq 6.84$ (value of N for R1). By comparing the MIC_a values of the 97 peptides of Robinson et al.³³ to their Q and N descriptors, we can see that in general this rule holds although numerous exceptions do exist.

The best QSAR model of the haemolytic effect for the R1 analogues relates the lysis of human red blood cells to the lipophilicity of the nonpolar face, N (Fig. 4):

$$\log\%Hem = -2.551 + 0.431 \cdot N \quad (2)$$

($n = 97$, $LOF = 0.077$, $R^2 = 0.694$, $R_{cv}^2 = 0.679$, F -test = 179.18, $\sigma = 0.136$, $\alpha > 95\%$, $n_o = 15$). The model suggests that the haemolytic potency of R1 analogues depends primarily on the lipophilicity of the nonpolar face and is almost independent on the charge and composition of the polar face. This is not surprising since the outer leaflet of mammalian cells is composed predominantly of neutral (zwitterionic) phospholipids^{8,9} in contrast to the anionic surfaces of bacterial

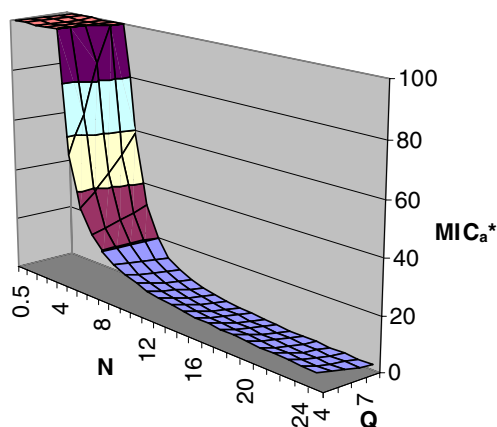


Figure 3. Dependence of MIC_a on charge and lipophilicity of the nonpolar face. The MIC_a dependence on molecular charge (Q) and the lipophilicity of the nonpolar face (N) was prepared by plotting the regression equation $MIC_a = 10^{(1.291 - 0.180 \cdot Q + 1.438 \cdot Q/N)}$. The colouring scheme helps to discriminate between MIC_a ranges.

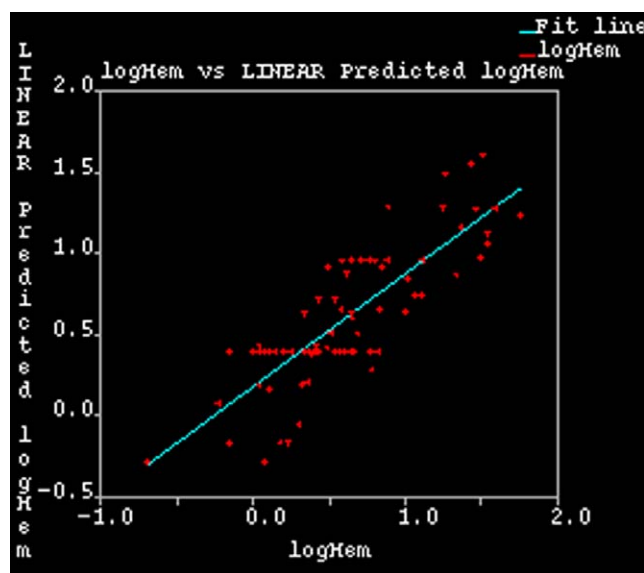


Figure 4. QSAR model of haemolytic effect of cationic peptides—R1 analogues. The resulting regression equation: $\log\%Hem = -2.551 + 0.431 \cdot N$ ($n = 97$, $R^2 = 0.69$, $R_{cv}^2 = 0.68$, F -test = 179.18, $\sigma = 0.136$, $\alpha > 95\%$, $n_o = 15$) relates the percentage of haemolysis of human red blood cells to the lipophilicity of the nonpolar face of the peptides (N). Figure was obtained by QSAR module of Cerius^{2,36}.

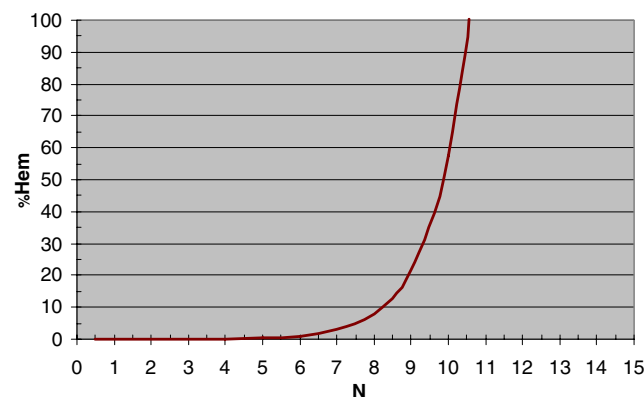


Figure 5. Dependence of %Hem on lipophilicity of nonpolar face. Dependence of the percentage of haemolytic activity (%Hem) in [%] at the peptide concentration of 100 μ g/mL on the lipophilicity of the nonpolar face (N) of R1 analogues.

membranes.^{32,38} The plot of %Hem against N indicates that the haemolytic potency of the analogues is almost negligible for $N \leq 6$ but increases strongly for $N \geq 8.5$ (Fig. 5). Based on this QSAR model, any analogue with $N \leq 6.84$ should show lower levels of haemolytic activity than the lead peptide R1. Inspection of the %Hem values of the 97 peptides of Robinson et al.³³ shows that this general trend is preserved by most of the peptides although some exceptions do exist.

2.2. Optimisation of antimicrobial and haemolytic effects

Simultaneous optimisation of the antimicrobial and haemolytic effects of R1 analogues is possible as both these bioactivities depend strongly on the lipophilicity

of the nonpolar face and an interval of N exists in which both the desired bioactivity and the harmful side effect reach acceptable levels (Fig. 6), approximately $7.5 \leq N \leq 8.5$. It should be emphasised here that the two QSAR models represent only a relatively gross simplification of the complex relationship between the bioactivities and the molecular properties of the peptides with a restricted accuracy of the predictions. For example, the regression Eqs. 1 and 2 assign to R1 with $Q = 7e$ and $N = 6.84$ values of $MIC_a = 31.9 \mu\text{g/mL}$ and $\%Hem = 2.5\%$, while the experimental values are lower with $10.4 \mu\text{g/mL}$ and 1.4% .

Utilization of the presented QSAR models based on molecular properties for the design of new antimicrobial peptides is also somewhat limited since it does not provide unique guidelines for translation of the optimum molecular properties into new sequences. Nevertheless, the combination of the QSAR molecular property–bioactivity models with the cyclic backbone of the protegrin analogues (constant turns, residues 6, 7 and 13, 14—Fig. 1), sequence amphipathicity (regular alternation of cationic and nonpolar residues) and peptide symmetry provides a sufficient strategy for the peptide design. For example, the opposite trends of the dependence of the antimicrobial and haemolytic effects on N can be illustrated on case sequences of symmetric cyclic PG-1 and R1 analogues with eight cationic residues ($Q = 8e$) and an ideal amphipathic

structure (Fig. 7), Table 5. Inspection of the predicted antimicrobial (MIC_a^*) and haemolytic ($\%Hem^*$) potencies for sequences NR1–NR17 calculated from the regression Eqs. 1 and 2 shows that peptides NR7–NR9 with homogeneous nonpolar faces formed entirely by less lipophilic aliphatic norvalines, valines or methionines, may constitute cationic peptides with optimised potencies of the desired and the side effects. The secondary structure of the backbone of the peptides NR7–NR9 is stabilised by a Cys₃–Cys₁₀ disulfide bridge in the form of a cyclic β -hairpin. Tam et al.¹⁴ showed by circular dichroism experiments that cyclic protegrins containing one to three cysteine bonds display some degree of β -strand structure in solutions. Recently, it was reported that the presence of the β -hairpin fold is essential for the membrane permeation/disruption by PG-1 analogues.^{14,27,31} PG-1 variants missing the cross-links and noncovalent conformation-stabilising features acquire namely random structures in solution.^{27,31}

3. Conclusions

We have analysed 97 cyclic cationic sequences of PG-1 mimetics of Robinson et al.³³ in terms of molecular properties and derived QSAR models that explain the observed variance of their averaged antimicrobial effect with 60% accuracy and haemolytic side effect with 68% accuracy. According to these relatively simple models, the antimicrobial effect is proportional to the overall molecular charge Q and the amphipathicity index Q/N (i.e., is inversely proportional to the lipophilicity of the nonpolar face, N), while the haemolytic effect is directly proportional to N . Therefore, it is possible to simultaneously optimise (decouple) these two concurrent effects by site-directed residue substitutions in the nonpolar face of the cyclic peptides so that its lipophilicity falls into the narrow range of: $7.5 \leq N \leq 8.5$. This can be achieved by numerous combinations of nonpolar amino acids. One specific example of such sequences spanning a range of N for an ideal amphipathic cyclic scaffold resembling the R1 and PG-1 is given. These sequences contain homogeneous symmetric nonpolar faces composed of mildly lipophilic residues. The most interesting sequences, NR7–NR9, include also a disulfide bridge that stabilises the cyclic backbone into the form of a constrained β -hairpin structure. An experimental study of this example (perhaps by Robinson et al.) would be interesting and appreciated.

It is now relatively well accepted that antimicrobial effect of the cationic peptides depends on their positive charge and amphipathic structure. However, the strategy of simultaneous modulation of the antimicrobial and haemolytic potencies of cationic β -hairpin peptides by specific substitutions in the nonpolar face represents a relatively novel finding,²³ which deserves further attention. It may namely help to overcome the serious problem of the haemolytic side effect of potent cationic antimicrobial peptides, which hampers them from entering into the drug development pipeline.

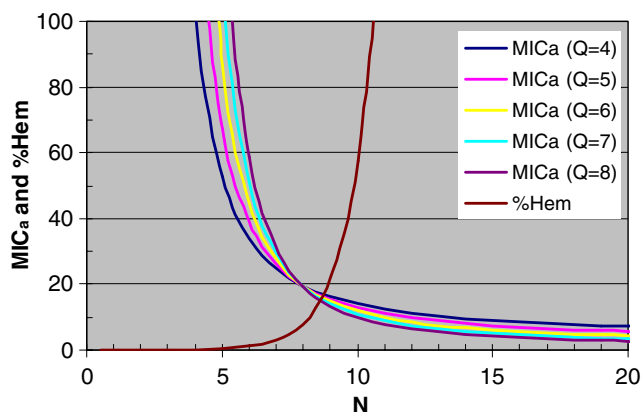


Figure 6. Dependence of MIC_a and $\%Hem$ on charge and lipophilicity of nonpolar face. Cross-sections of the surface $MIC_a = f\{Q, N\}$ in micrograms per milliliter (Fig. 4) at points $Q = 4e - 8e$ and dependence of percentage of haemolytic activity ($\%Hem$) in [%] on the lipophilicity of the nonpolar face (N) of R1 analogues.

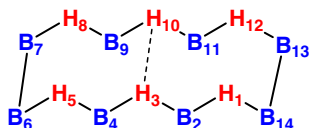


Figure 7. Cyclic β -hairpin peptides with ideal amphipathic structure—analogs of PG-1 and R1. Ideal amphipathic β -hairpin-like structure formed by regularly spaced hydrophobic residues (H) and cationic residues (B) bears a total charge of $Q = 8e$. Alternatively, the cyclic backbone can be constrained in a β -hairpin conformation by a Cys₃–Cys₁₀ disulfide bridge.

Table 5. Example of symmetric cationic peptide sequences with ideal amphipathic cyclic β -hairpin structure

Pep. ^a	P.1	P.2	P.3	P.4	P.5	P.6	P.7	P.8	P.9	P.10	P.11	P.12	P.13	P.14	Q^b (e)	N^c	MIC _a ^{*d} ($\mu\text{g/mL}$)	%Hem ^{*e} (%)
NR1	Tyr	Arg	Tyr	Lys	Tyr	Arg	Arg	Tyr	Lys	Tyr	Arg	Tyr	Arg	Arg	8	5.76	70.7	0.9
NR2	Tyr	Arg	Val	Lys	Tyr	Arg	Arg	Tyr	Lys	Val	Arg	Tyr	Arg	Arg	8	6.28	48.3	1.4
NR3	Tyr	Arg	Tle	Lys	Tyr	Arg	Arg	Tyr	Lys	Tle	Arg	Tyr	Arg	Arg	8	6.62	38.9	2.0
NR4	Val	Arg	Tyr	Lys	Val	Arg	Arg	Val	Lys	Tyr	Arg	Val	Arg	Arg	8	6.80	35.0	2.4
NR5	Nva	Arg	Val	Lys	Nva	Arg	Arg	Nva	Lys	Val	Arg	Nva	Arg	Arg	8	7.20	28.2	3.6
NR6	Nva	Arg	Tle	Lys	Nva	Arg	Arg	Nva	Lys	Tle	Arg	Nva	Arg	Arg	8	7.54	23.8	4.9
NR7	Nva	Arg	Cys	Lys	Nva	Arg	Arg	Nva	Lys	Cys	Arg	Nva	Arg	Arg	8	7.84	20.9	6.7
NR8	Val	Arg	Cys	Lys	Val	Arg	Arg	Val	Lys	Cys	Arg	Val	Arg	Arg	8	7.96	19.8	7.6
NR9	Met	Arg	Cys	Lys	Met	Arg	Arg	Met	Lys	Cys	Arg	Met	Arg	Arg	8	8.00	19.5	7.9
NR10	Nva	Arg	Leu	Lys	Nva	Arg	Arg	Nva	Lys	Leu	Arg	Nva	Arg	Arg	8	8.16	18.3	9.3
NR11	Nva	Arg	Nle	Lys	Nva	Arg	Arg	Nva	Lys	Nle	Arg	Nva	Arg	Arg	8	8.28	17.4	10.4
NR12	Nva	Arg	Ile	Lys	Nva	Arg	Arg	Nva	Lys	Ile	Arg	Nva	Arg	Arg	8	8.36	16.9	11.3
NR13	Val	Arg	Ile	Lys	Val	Arg	Arg	Val	Lys	Ile	Arg	Val	Arg	Arg	8	8.48	16.2	12.7
NR14	Tle	Arg	Cys	Lys	Tle	Arg	Arg	Tle	Lys	Cys	Arg	Tle	Arg	Arg	8	8.64	15.2	14.9
NR15	Tle	Arg	Leu	Lys	Tle	Arg	Arg	Tle	Lys	Leu	Arg	Tle	Arg	Arg	8	8.96	13.7	20.5
NR16	Nva	Arg	Trp	Lys	Nva	Arg	Arg	Nva	Lys	Trp	Arg	Nva	Arg	Arg	8	9.26	12.4	27.6
NR17	Leu	Arg	Leu	Lys	Leu	Arg	Arg	Leu	Lys	Leu	Arg	Leu	Arg	Arg	8	10.20	9.5	70.3

Cha, L-cyclohexylalanine; Chah, L-homocyclohexylalanine; Hfe, L-homophenylalanine; Nal1, L-1-naphthylalanine; Nal2, L-2-naphthylalanine; Cif, L-4-chlorophenylalanine; Bip, L-4-biphenylalanine; Orn, L-ornithine; Trb, L-(*O*-benzyl)tyrosine; Cit, L-citrulline; Nle, L-norleucine; Seb, L-(*O*-benzyl)serine; Nva, L-norvaline; Tle, L-*tert*-leucine; Abu, L-2-aminobutyric acid.

^a The peptides with sequences P.1–P.14 are based on the analogy with the lead peptide R1.³³ For numbering of residues, see Figure 7.

^b Molecular charge Q was calculated as the sum of formal side-chain charges of all residues, in units of electron charge (e).

^c Lipophilicity of nonpolar face N was calculated as the sum of side-chain lipophilicities (π_{FP}) over residues forming the nonpolar face (Fig. 7), for details, see Section 4. Maximum range of N for a lipophilic face of the cyclic scaffold on Figure 7, which contains six nonpolar residues, is $0.78 \leq N \leq 22.56$.

^d Predicted averaged minimal inhibitory concentration MIC_a^{*} was calculated from the regression Eq. (1): $\text{MIC}_a^* = 10^{(1.291 - 0.180 \cdot Q + 1.438 \cdot Q/N)}$, in units micrograms per milliliter.

^e Predicted percentage of haemolysis of human red blood cells %Hem^{*} at peptide concentration of 100 $\mu\text{g/mL}$ was calculated from the regression Eq. 2: $\% \text{Hem}^* = 10^{(-2.551 + 0.431 \cdot N)}$, in [%].

4. Methods

4.1. Molecular descriptors

Molecular descriptors used in the QSAR analysis of the peptides were defined as additive parameters obtained by summing up the contributions of residues either by including the whole sequence or only the residues forming the polar or nonpolar face of the cyclic β -hairpin (Fig. 1).

Molecular charge of the peptides was calculated as $Q = \sum_i^{\text{all}} q_i$, where q_i is the formal charge of a residue at the pH of 7, which depends on the pK_a constant of its side chain.³⁹ Hydrophobicity/lipophilicity parameters, L , P and N , were defined via residue side-chain lipophilicity parameter, π_{FP} , of Fauchere and Pliska,⁴⁰ as a summation over all residues of the peptide (L) or over residues forming the polar (P) or nonpolar (N) face as, for example, $N = \sum_i^{\text{nonp}} \pi_{FPi}$. The π_{FP} parameter represents the difference between experimental partitioning coefficients in *n*-octanol/water system, $\log P_{o/w}$, of a given amino acid and glycine: $\pi_{FP} = \log P_{o/w}(\text{a.a.}) - \log P_{o/w}(\text{Gly})$, (Table 3). For unusual amino acids the π_{FP} parameters were obtained by a linear regression fitting of π_{FP} to π_{CLOGP} for the training set of 20 natural amino acids: $\pi_{FP} = 1.070936 \cdot \pi_{CLOGP} - 0.02784$ (number of samples $n = 20$, squared correlation coefficient $R^2 = 0.91$, leave-one-out cross-validated correlation coefficient $R_{\text{vx}}^2 = 0.90$, Fischer test F -test = 165.5, standard deviation $\sigma = 0.43$, level of sta-

tistical significance $\alpha > 95\%$) and interpolation/extrapolation of the linear dependence. The index π_{CLOGP} was calculated for all considered amino acids by the CLOGP program,⁴¹ which uses a molecular fragment method of the $\log P_{o/w}$ estimate, as $\pi_{CLOGP} = \text{CLOGP}(\text{a.a.}) - \text{CLOGP}(\text{Gly})$.

Bulkiness of peptides was expressed via surface areas of the analogues and their two faces, which were calculated as the sum of side-chain surface areas over residues forming the polar (S_P) and nonpolar face (S_N), as for example, $S_N = \sum_i^{\text{nonp}} S_i$ and $S = S_P + S_N$. The residue side-chain surface area was calculated as $S_i = S_{\text{Con}}(\text{a.a.}) - S_{\text{Con}}(\text{Gly})$, using the Connolly surface calculation method⁴² of Insight-II modelling package⁴³ with a probe radius of 1.4 Å, surface point density of 30 points/Å². The amino acids modelled in an fully extended conformation were minimized with CFF91 force field⁴⁴ by Newton–Raphson method assuming a convergence threshold of the gradient of 0.001 kcal/(mol Å) and dielectric constant of 80 to mimic the effect of solvent upon the side-chain conformation.⁴³ Molecular weights of the analogues (M_w , M_{wP} and M_{wN}) were computed as the sum of the relevant residue contributions. Count of small lipophilic residues (C_{SL}), highly lipophilic residues (C_{HL}) and aromatic residues (C_{AR}) within the nonpolar face was also considered.

Amphipathicity descriptors were defined as the ratio of molecular properties that characterize the whole peptide

and/or its polar and nonpolar faces: P/L , P/N , L/N , Q/L , Q/N , S_P/S_N , M_{WP}/M_{WN} , Q/C_{SL} , Q/C_{HL} and Q/C_{AR} (Table 3).

Flexibility of the peptide was approximately expressed via total number of rotatable (single nonaromatic) bonds in the side chains as: $RotBon = \sum_i^{all} R.B._i$, where $R.B._i$ is the number of rotatable bonds in an amino acid side chain: $R.B._i = R.B.(a.a.) - R.B.(Gly)$.

4.2. Bioactivity data

The minimal inhibitory concentrations (MICs) against Gram-negative and Gram-positive bacterial strains (*E. coli*, *P. aeruginosa* and *S. aureus*) and the percentage of haemolysis of human red blood cells (%Hem) at the concentration of 100 µg/mL of the 97 cationic peptides considered were taken from Robinson et al.³³ The MIC values averaged over the panel of bacterial strains tested (MIC_a) were used to facilitate the assessment of the overall antimicrobial effect of the PG-1 analogues which display activity against a wide range of bacteria, yeast and fungi.^{14,25–27}

4.3. Generation of QSAR models and statistical analysis

The space of possible QSAR models on the set of molecular descriptors considered was sampled by the genetic function approximation (GFA) algorithm³⁵ of the Cerius² package³⁶ using the Friedman's lack-of-fit (LOF) score³⁷ to estimate the fitness of each model.

In the GFA, progeny populations of QSAR models are created by evolving a random initial population of equations constructed from the set of available descriptors by standard regression techniques, using the genetic algorithm. The genetic algorithm automatically selects the type and number of descriptors to be used in the models by combining (crossing-over) equations with the best fitness scores as good combinations of genes (i.e., descriptors) are expected to lead to improved models in the resulting offspring population of equations.

For both antimicrobial and haemolytic activity data the analyses started by building of a population of 500 randomly constructed linear equations containing combinations of three descriptor terms. The initial population was then evolved for 50,000 generations with a variable equation length and mutation probabilities set at: (i) adding new term 50%, (ii) reducing number of terms 50% and (iii) extending number of terms 50%. The smoothness parameter was set to 2.0 to bias the equation scoring and evolution towards smaller number of terms, that is, more compact and easier to interpret QSAR models. Least-squares regression method was used to generate the QSAR equations for the sampled combinations of descriptors. At the end, the final population of regression equations was ranked based on the LOF score and the best scoring QSAR models were subjected to removal of outliers and leave-one-out cross-validation.

References and notes

- Beisswenger, C.; Bals, R. *Curr. Protein Pept. Sci.* **2005**, *6*, 255–264.
- Park, Y.; Hahm, K. S. *J. Biochem. Mol. Biol.* **2005**, *38*, 507–516.
- Hancock, R. E. W. *Drugs* **1999**, *57*, 469–473.
- Mosca, D. A.; Hurst, M. A.; So, W.; Viajar, B. S. C.; Fujii, C. A.; Falla, T. J. *Antimicrob. Agents Chemother.* **2000**, *44*, 1803–1808.
- Shai, Y. *Biopolymers* **2002**, *66*, 236–248.
- Andres, E.; Dimarcq, J. L. *J. Int. Med.* **2004**, *255*, 519–520.
- Chen, J.; Falla, T. J.; Liu, H.; Hurst, M. A.; Fujii, C. A.; Mosca, D. A.; Embree, J. R.; Loury, D. J.; Radcl, P. A.; Cheng Chang, C.; Gu, L.; Fiddes, J. C. *Biopolymers* **2000**, *55*, 88–98.
- Hwang, P. M.; Vogel, H. J. *Biochem. Cell. Biol.* **1998**, *76*, 235–246.
- Oren, Z.; Shai, Y. *Biopolymers* **1998**, *47*, 451–463.
- Huang, H. W. *Biochemistry* **2000**, *39*, 8347–8352.
- Roumestand, C.; Louis, V.; Aumelas, A.; Grassy, G.; Calas, B.; Chavanieu, A. *FEBS Lett.* **1998**, *421*, 263–267.
- Brogden, K. A. *Nat. Rev. Microbiol.* **2005**, *3*, 238–250.
- Kondejewski, L. H.; Jelokhani-Niaraki, M.; Farmer, S. W.; Lix, B.; Kay, C. M.; Sykes, B. D.; Hancock, R. E. W.; Hodges, R. S. *J. Biol. Chem.* **1999**, *274*, 13181–13192.
- Tam, J. P.; Wu, C.; Yang, J.-L. *Eur. J. Biochem.* **2000**, *267*, 3289–3300.
- Muhle, S. A.; Tam, J. P. *Biochemistry* **2001**, *40*, 5777–5785.
- Shai, Y. *Curr. Pharm. Des.* **2002**, *8*, 715–725.
- Lee, D. L.; Hodges, R. S. *Biopolymers* **2003**, *71*, 28–48.
- Powers, J. P.; Hancock, R. E. *Peptides* **2003**, *24*, 1681–1691.
- Ganz, T. *Nat. Rev. Immunol.* **2003**, *3*, 710–720.
- Lohner, K.; Blondelle, S. E. *Comb. Chem. High Throughput Screening* **2005**, *8*, 241–256.
- Strøm, M. B.; Haug, B. E.; Skar, M. L.; Stensen, W.; Stiberg, T.; Svendsen, J. S. *J. Med. Chem.* **2003**, *46*, 1567–1570.
- Lejón, T.; Stiberg, T.; Strøm, M. B.; Svendsen, J. S. *J. Pept. Sci.* **2004**, *10*, 329–335.
- Frečer, V.; Ho, B.; Ding, J. L. *Antimicrob. Agents Chemother.* **2004**, *48*, 3349–3357.
- Ostberg, N.; Kaznessis, Y. *Peptides* **2005**, *26*, 197–206.
- Kokryakov, V. N.; Harwig, S. S.; Panyutich, E. A.; Shevchenko, A. A.; Aleshina, G. M.; Shamova, O. V.; Korneva, O. V.; Lehrer, R. I. *FEBS Lett.* **1993**, *327*, 231–236.
- Miyasaki, K. T.; Lehrer, R. I. *Int. J. Antimicrob. Agents* **1998**, *9*, 269–280.
- Lai, J. R.; Huck, B. R.; Weisblum, B.; Gelman, S. H. *Biochemistry* **2002**, *41*, 12835–12842.
- Albrecht, M. T.; Wang, W.; Shamova, O. V.; Lehrer, R. I.; Schiller, N. L. *Respir. Res.* **2002**, *3*, 18–28.
- Gidalevitz, D.; Ishitsuka, Y. J.; Muresan, A. S.; Kononov, O.; Waring, A. J.; Lehrer, R. I.; Lee, K. Y. C. *Proc. Natl. Acad. Sci. U.S.A.* **2003**, *100*, 6302–6307.
- Buffy, J. J.; Hong, T.; Yamaguchi, S.; Waring, A. J.; Lehrer, R. I.; Hong, M. *Biophys. J.* **2003**, *85*, 2363–2373.
- Mani, R.; Waring, A. J.; Lehrer, R. I.; Hong, M. *Biochim. Biophys. Acta* **2005**, *1716*, 11–18.
- Langham, A. A.; Khandelia, H.; Kaznessis, Y. N. *Biopolymers* **2006**, *84*, 219–231.
- Robinson, J. A.; Shankaramma, S. C.; Jetter, P.; Kienzl, U.; Schwenderer, R. A.; Vribloed, J. W.; Obrecht, D. *Bioorg. Med. Chem.* **2005**, *13*, 2055–2064.
- Wade, D.; Boman, A.; Wählin, B.; Drain, C. M.; Andreu, D.; Boman, H. G.; Merrifield, R. B. *Proc. Natl. Acad. Sci. U.S.A.* **1990**, *87*, 4761–4765.

35. Rogers, D.; Hopfinger, A. J. *J. Chem. Inf. Comput. Sci.* **1994**, *34*, 854–866.
36. Cerius² Life Sciences, version 4.5, Accelrys, San Diego, CA, 2000.
37. Friedman, J. Multivariate Adaptive Regression Splines, Technical Report 102, Laboratory for Computational Statistics, Department of Statistics, Stanford University: Stanford, CA (1988; revised 1990).
38. Boman, H. G. *Annu. Rev. Immunol.* **1995**, *13*, 61–92.
39. Dawson, R. M. C.; Elliott, D. C.; Elliott, W. H.; Jones, K. M. *Data for Biochemical Research*, 3rd ed.; Oxford Science Publications, 1986, pp 1–31.
40. Fauchere, J. L.; Pliska, V. *Eur. J. Med. Chem.* **1983**, *18*, 369–375.
41. ClogP, Daylight Chemical Information Systems Inc., <http://www.daylight.com/>.
42. Connolly, M. L. *J. Appl. Crystallogr.* **1983**, *16*, 548–558.
43. Insight-II, version 2000 and Discover 2.98 molecular modelling and simulation package, Accelrys, San Diego, CA, 2000.
44. Maple, J. R.; Hwang, M. J.; Stockfish, T. P.; Dinur, U.; Waldman, M.; Ewing, C. S.; Hagler, A. T. *J. Comput. Chem.* **1994**, *15*, 162–182.
45. Kyte, J.; Doolittle, R. F. *J. Mol. Biol.* **1982**, *157*, 105–132.